Qeios

Experimental behavior of solar still using mixed oxides Mn-Fe/silicone resin composite as selective solar absorber

Carlos Juárez Salinas[a,*], **Reyna Ventura Reyes**[a], **Víctor Rentería Tapia**[b], **Carlos Fernández Rendón**[c], **Enrique Barrera Calva**[a].

[a]Department of Processes and Hydraulics, Division of Basic Sciences and Engineering. Iztapalapa Metropolitan Autonomous University, Av. San Rafael Atlixco 186, Col. Vicentina, C.P. 09340, Iztapalapa, México City, México.

[b]Department of Natural and Exact Sciences, Cuvalles-University of Guadalajara, Carretera Guadalajara-Ameca Km 45.5, C.P. 46600. Ameca Jalisco, México

[c]Ecotoxicology Laboratory, Department of Hydrobiology, Division of CBS, Iztapalapa Metropolitan Autonomous University, Av. San Rafael Atlixco 186, Col. Vicentina, C.P. 09340, Iztapalapa, México City, México.

*Correspondence: juarezsalce@gmail.com

Abstract.

In this research, the optical properties of a black pigment of mixed Mn-Fe oxides synthesized by the precipitation method dispersed in silicone resin at different concentrations for use as a solar absorber in a two-slope passive solar still were evaluated. The transmittance of different thicknesses of float glass with 0.1% Fe2O3 was also studied for use as a condenser in the construction of the solar still. Regarding the pigments, the absorbance and spectral emittance were evaluated, the floated. With the above information, both the absorbent surface and the condensers were optimized to propose the best design of the solar still. The novel hybrid material used as a selective coating in the still, which corresponds to 2.3% Mn-Fe mixed oxides, exhibited a high solar absorbance of 91.82% and a relatively low infrared thermal emission of less than 57.22%, as well as good stability to the corrosive and hot environment of the solar still, in addition to great durability over time and in real operating conditions. The float glass with the highest transmittance corresponds to a thickness of 3 mm and an average transmittance of 82.57%. The built prototype was characterized by obtaining the temperature profiles of the absorber and condensers, thermal efficiency, production and water quality. The prototype has a thermal efficiency of 29.6%, requiring only energy from the sun for its operation. The water produced by this device becomes an option for human use and consumption in accordance with current official standards, allowing supply in communities that do not have access to drinking water but have access to seawater or waters with high hardness.

Keywords: Solar absorber; Black mixed oxides; Mn-Fe Solar still; Water quality.

https://doi.org/10.32388/Z57AR1.2

Highlights

• Selective solar absorber based on the mixed oxides Mn-Fe/resin composite

• Design, construction and characterization of the solar still

• Thermal efficiency analysis of the device

• Distilled water quality analysis

Nomenclature

H	Insolation, [MJ / m^2]
I	Experimental Irradiance; [W / m^2]
$I_s(\lambda)$	Irradiance AM 1.5 G; [W / m^2]
T	Temperature; [K]

Greek letters

$\alpha(\lambda)$	Spectral absorptance [-]
α_s	Solar absorptance, [-]
$\varepsilon(\lambda)$	Spectral emittance [-]
ε_t	Thermal emittance; [-]
η	Thermal efficiency; [-]
$\tau(\lambda)$	Spectral transmittance; [-]
τ	Solar transmittance; [-]

Abbreviations

EC	Escherichia coli
pH	Hydrogen potential
MPN	Most Probable Number
TDS	Total Dissolved Solids, [mg/L]
BGBLB	Brilliant Green Bile Lactose Broth

1. Introduction

The water solar distillation for human consumption is today an attractive alternative since the distilled water by the action of solar energy is usually very pure; This technique has received considerable attention from the second half of the 20th century in many regions of the world where seawater is abundant, drinking water is scarce and solar irradiation is high. Even today, due its versatility, solar distillation has had a growing interest in recent years [1].

Nature itself, based on the water cycle that the oceans follow, is a clear example of how to obtain drinking water by means of solar stills. Being solar distillation, the path that the planet's water follows to carry out its cycle, it is reliable to emulate this process to obtain drinking water from seawater or brackish water using these prototypes.

The equipment used to distill water using solar radiation (either passively or actively) is called solar stills, which are useful in hot climates and with a high annual average solar irradiation. The water production depends to a great extent on the dimensioning of the device and the materials used in its manufacture, so improvements are feasible in terms of its efficiency and the total daily water production [2]. Regarding the dimensioning and components, solar stills have many shapes and the materials used in their manufacture are wide, but in all, the distillation process is quite similar. Among the main designs, can be found single-slope solar stills, in the form of a house (also called Australian or two-slope), multiple-effect, those that are greenhouse type, pyramid-shaped [3], those that use solar concentrators [4], those with an inclined tray [5], as well as those that are tubular [6] and in a spherical shape [7], among others. Most use different types of glass or acrylic as a collector cover; in addition, the collecting tubs can be made of glass, fiberglass, acrylic, rubber [8], steel, and there are even some prototypes that are made of ferrocement [9]. In addition, different types of solar radiation absorbing surfaces can be mentioned in terms of their structure that can be conventional, with fins or corrugated absorbers surfaces, among others [10]. Insulating materials are of many types as well and among them, we can mention glass wool, cardboard, and polyurethane, among others [11].

As noted above, various technological materials with specific optical and thermal properties are required in the fabrication of these photothermal systems. In particular, the selective absorber coatings deposited on metallic substrates play an important role in the efficiency of the photothermal conversion of the solar radiation. Solar absorber surfaces ideally should exhibit high thermal and chemical stability, high absorptance (>0.95) in the wavelength range from 0.3 up to 2.5 μm and low emittance (<0.10) in the infrared region (2.5-25 μm) at the operating temperature of the device. In order to achieve these requirements a variety of selective absorber coatings and paints have been produced [12]. Specifically, the metal-oxide/dielectric composites have showed good thermal performance at low-cost and in particular, as the dielectric is an organic medium such as silicone resin. Generally, the resins have low electrical and thermal conductivity, although these properties are notably improved by using absorber pigments for solar thermal applications. The particle size, concentration, thickness of the coatings and dispersion of the pigment has an important effect on the solar optical properties [13]. One the most popular pigments is Fe_2O_3:Mn, which is composed by crystalline hematite and bixbyite phases, exhibiting high solar absorptance in the 0.75 to 0.94 range and low emittance in the range of 0.03 to 0.07 [13]. Similarly, high transparence

in the solar spectrum of the condenser covers is required to favor the greenhouse effect in the solar still.

Improving the configuration of conventional solar stills to increase productivity has always been the concern of engineers and researchers in the field of solar energy and related topics. The time-consuming and expensive manufacturing processes of solar stills motivate researchers to perform mathematical and computational fluid dynamics (CFD) simulations of solar stills to estimate productivity [14]. The literature review reveals that many other studies can be carried out in the future on the CFD simulation of solar stills in which various techniques such as the use of nanotechnology, best reflectors, storage materials, fans and fins have been considered to improve the efficiency of the solar desalination systems [15].

Referring to the current problems in Mexico, there are several places far from the cities that lack drinking water, but that have hard or brackish water both superficially, underground and maritime that could be used through purification methods that are economically viable and consistent with the environmental. According to the National Water Program 2014-2018 [16], almost nine million people lack drinking water (five million are in rural areas) and 11 million lack sewerage (7.8 million in rural areas), making it essential to address the problem of water shortage, becoming essential to use solar energy seriously, when appropriate, to desalinate seawater, in places where unique hydrological, geographical, and physical conditions exist with competitive costs.

2. Materials and methods

The synthesis of iron-manganese oxides used as solar selective coating was carried out by the co-precipitation method. They were prepared by using the precursors $FeCl_3 \cdot 6H_2O$ (97%) and $MnCl_2 \cdot 4H_2O$ (97 %) purchased from Sigma-Aldrich. Both salts were dissolved in deionized water and mixed in the appropriate amount to obtain the desired molar ratio of Fe / Mn= 1/3. The stoichiometry ratio between Fe and Mn strongly influences on the optical properties of the composites. The mixture was precipitated using a concentrated solution of sodium hydroxide NH_4OH (28%, Sigma-Aldrich) under stirring at a temperature of 60 °C. Throughout the precipitation process, the pH was maintained above 10. The resulting precipitated was washed several times with distilled water and calcined at 800 °C for 1 h. Once the oxides have been obtained, they were mixed with commercial acetic silicone from Sista trademark at different concentrations in the range from 2.3-13% wt to determine the one with the highest solar absorptance and low emittance. This silicone is transparent with a density of 1.02 g/ml, extrusion of 370 g/ml, elongation of 480% and a curing time of 24 h. Similarly, in order to optimize the transmittance of the condenser cover made of glass, different thickness of this material was considered. Afterwards the optimization of the better materials for the construction of the solar still, the metal-oxide/resin hybrid material was applied in a thin film on the metal substrate of the distiller by means of a stiff bristle brush, leaving an absorbing layer in the order of 300 μm thick.

For the characterization of the condenser (float glass with 0.1% of Fe_2O_3), their transmittance in the solar region (300 to 2500 nm) was evaluated with a Varian 5E UV-Vis-NIR spectrophotometer and an integration was made over the solar region to obtain the

average values of the transmittance of each condenser candidate. The expression that allows the average transmittance to be derived from the spectrum transmittance is [17]:

$$\tau = \frac{\int I_s(\lambda)\tau(\lambda)d\lambda}{\int I_s(\lambda)d\lambda} \qquad (1)$$

Where λ is the wavelength, $\tau(\lambda)$ is the spectral transmittance and $I_s(\lambda)$ is the normal solar irradiance, corresponding to the AM 1.5 G.

The crystal structure of the solar absorber samples was obtained through X-ray diffraction patterns on a Bruker D8 Advance diffractometer with Cu-Kα radiation, operating in Bragg-Brentano geometry. Patterns were obtained in an interval of 15° to 108° in 2θ with a step of 0.020414° and 76.8 s per point.

The spectral reflectance of black pigments in the range of 300 to 2500 nm was obtained from a Varian 5E UV-Vis-NIR spectrophotometer using an integration sphere. Once spectral reflectance $\rho(\lambda)$ has been obtained, spectral absorptance can be found through the formula [18] $\alpha(\lambda) = 1 - \rho(\lambda)$, considering that the system is in thermal equilibrium. Average absorptance is obtained through expression [17,18]:

$$\alpha_s = \frac{\int I_s(\lambda)\alpha(\lambda)d\lambda}{\int I_s(\lambda)d\lambda} \qquad (2)$$

Where λ is the wavelength, $\alpha(\lambda)$is the spectral absorptance and $I_s(\lambda)$ is the normal solar irradiance, ideally corresponding to the AM 1.5 G.

The spectral reflectance $\rho(\lambda)$ of the samples in the range of 2500-25000 nm was obtained using a Nicolet iS50 FT-IR spectrophotometer. The spectral emittance is obtained from the expression [18] $\varepsilon(\lambda) = 1 - \rho(\lambda)$

The average emittance is derived from the expression [17,18]:

$$\varepsilon_t = \frac{\int E(\lambda,T)\varepsilon(\lambda)d\lambda}{\int E(\lambda,T)d\lambda} \qquad (3)$$

Where $E(\lambda,T)$ represents the Planck blackbody emission spectrum at 120 °C and whose expression is:

$$E(\lambda,T) = \frac{c_1}{\lambda^5\left(e^{\frac{c_2}{\lambda T}} - 1\right)} \qquad (4)$$

Being $c_1 = 3.7405x10^{20}\ Wnm^4m^{-2}$ and $c_2 = 1.43879x10^7\ nm\,K$.

In the case of surface profilometry, a Stylus Bruker Dektak XT profilometer was used to sweep an area of dimensions of 1 mm x 1 mm to determine the roughness of the samples and to obtain a three-dimensional image of each sample.

The efficiency of the still [19] is the relationship between the useful heat $\int_o^t qdt$ throughout the day and the total insolation H received:

$$\eta = \frac{\int_o^t q\, dt}{H} \cdot 100 \qquad (5)$$

Where H, the daily insolation is given by

$$H = \int_o^t Idt \qquad (6)$$

and where I is the experimentally observed irradiance.

Regarding the water quality study, the input water to the module and the output water were compared with respect to the permissible limits, characterizing the odor, flavor, pH, hardness, total. dissolved solids, salinity, total coliforms and fecal coliforms.

To measure the pH of the inlet and outlet water, a high-precision Webat portable pH meter was used; hardness was determined using a HACH 5-B hardness test kit; total dissolved solids using a Hanna Instruments HI98302 total dissolved solids meter with a high range that can measure up to 10.00 g/L; finally, salinity was evaluated in an Atago ATC-S/Mill-E refractometer.

3. Results and discussion

In order to optimize the performance of the solar still, different variables related to the crystal structure, the optical properties of the materials used for the construction of the solar still as well as their morphology were studied. The thickness of the collector glass cover, the influence of the concentration of mixed Mn-Fe oxides dispersed in the silicone resin on the absorption and emittance and morphology of the samples were considered.

3.1. Crystal Structure

Fig. 1 shows the diffraction patterns of the mixed oxides of Mn-Fe, these coincide with the reflection maxima reported in the ICDD-PDF 04-016-1434, ICDD-PDF 04-024-5003 and ICDD-PDF 01-074-9811 cards and correspond to the $MnFeO_3$, $Mn_{0.2}Fe_{2.8}O_4$ and $Fe_{0.84}Mn_{1.16}O_3$, all these oxides with cubic structure.

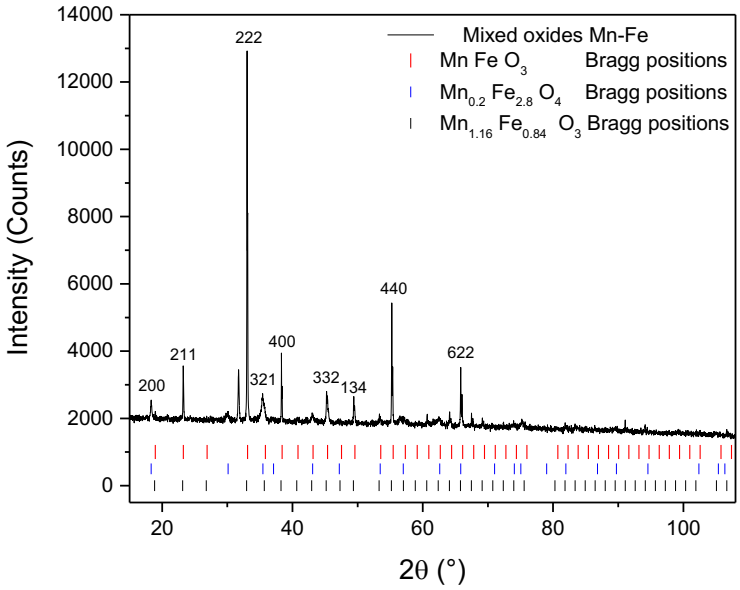

Fig. 1 Diffraction pattern of Mn-Fe oxides. The pattern shows a mixed composition of phases and the Bragg indices corresponding to the predominant phase $MnFeO_3$.

3.2. Optical properties

The transparent cover of different thickness with 0.1% Fe_2O_3 in the range of 300 to 2500 nm has been characterized (Fig. 2), obtaining an average weighted transmittance of 82.59% for the 3 mm thick glass cover. Table 1 shows the average transmittance for different thicknesses of float glass.

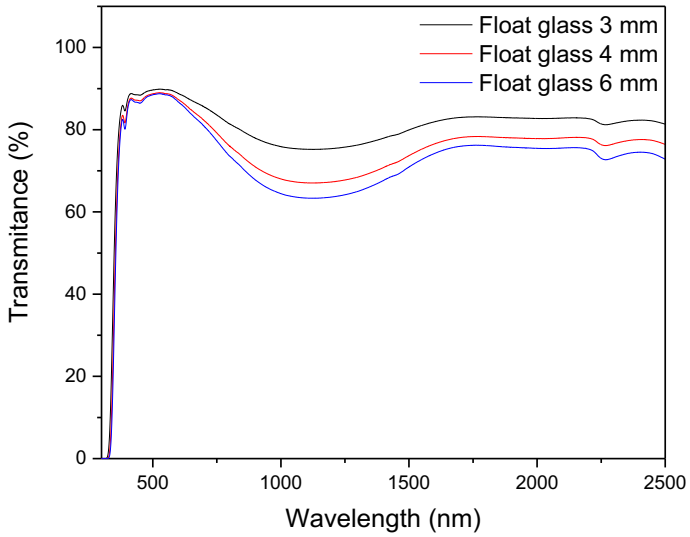

Fig. 2 Spectral transmittance of 0.1% Fe2O3 float glass with different thicknesses. The condenser with the highest transmittance corresponds to the one that has a thickness of 3 mm.

Table 1 Average transmittance values for different thicknesses of float glass with 0.1% Fe_2O_3.

Condenser	τ (%)
3 mm	82.59
4 mm	78.43
6 mm	76.58

On the other hand, the highest average solar absorption of 91.82% was achieved in the range of 300 to 2500 nm for Mn-Fe pigment oxides at a concentration of 2.3 % by weight (Fig. 3). The spectral emittance for different concentrations of Mn-Fe oxides is shown in Figure 4, the estimation of the emittance values for the MnFeO3/resin compound was 57.52% also at a concentration of 2.3%.

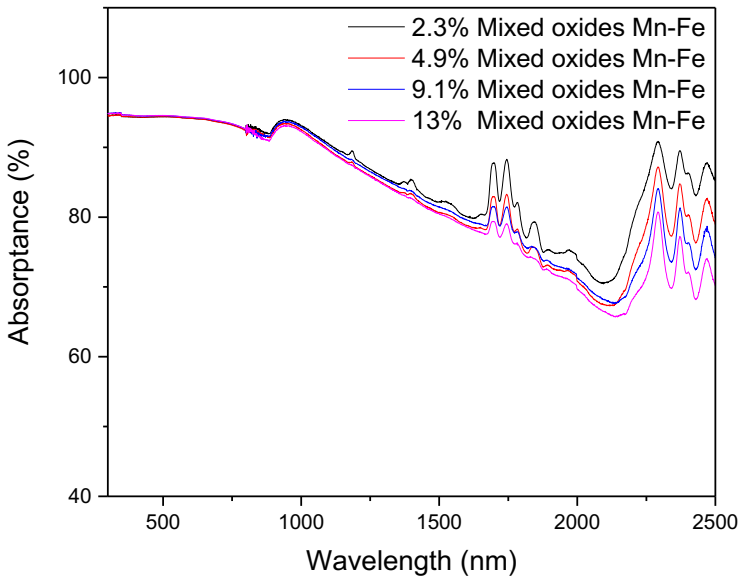

Fig. 3 Spectral solar absorptance for the powders of mixed oxides Mn-Fe in adhesive silicone at different concentrations.

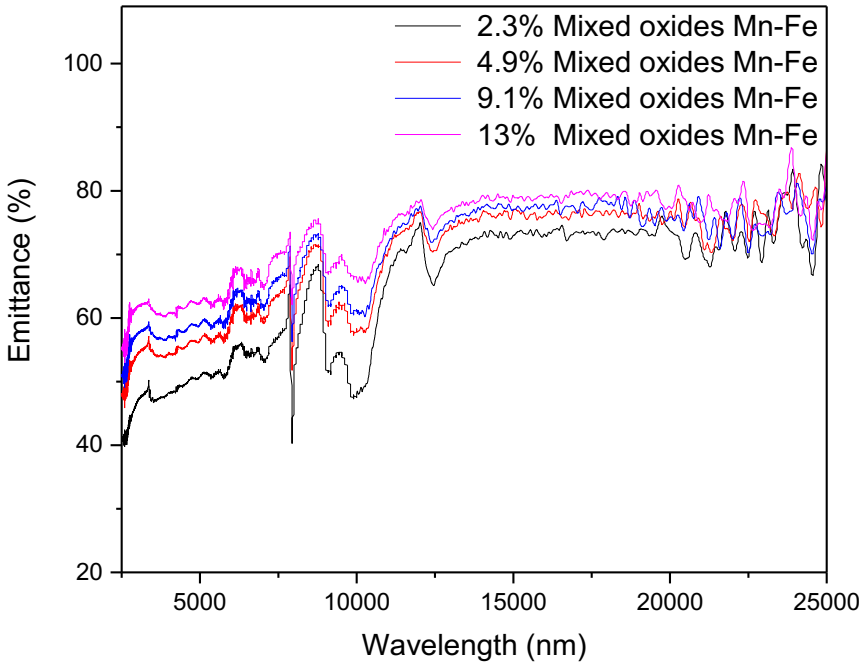

Fig. 4 Emittance for the powders of mixed oxides Mn-Fe in adhesive silicone at different concentrations.

Table 2 summarizes the value of absorption, emittance, and selectivity of each of the samples. As can be seen, the 2.3% sample exhibits the best optical behavior since it has the highest absorption and the lowest emittance.

Table 2. Values of the absorptance and emittance of each sample.

Sample	α (%)	ε (%)
2.3% Mixed oxides Mn-Fe	91.82	57.22
4.9% Mixed oxides Mn-Fe	91.29	62.98
9.1% Mixed oxides Mn-Fe	91.45	65.15
13% Mixed oxides Mn-Fe	91.12	68.39

3.3. Morphological properties

Through surface profilometry studies with the Stylus Bruker Dektak XT profilometer, three-dimensional images of the absorbent films have been obtained in areas of 1 mm^2 for each of the samples and their roughness has been obtained. Fig. 5 is an example image of the surface, obtaining roughness values of 4312.558 nm.

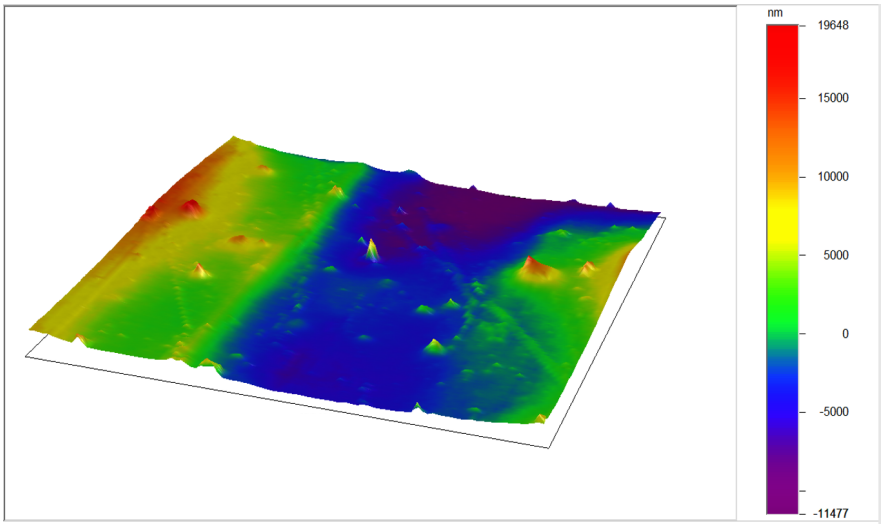

Fig. 5 Surface profilometry of Mn-Fe oxides in silicone in an area of 1 mm^2. The roughness is 4312.558 nm.

3.4. Construction solar still

After various tests on sizing and materials, an Australian type still was built (Fig. 6) with 1 m^2 of the solar radiation collection area and the condenser covers are made of clear glass. The transparent glass cover is 3 mm thick and has better transmittance (82.59%) compared with glass with mayor thickness, favoring the heat flow to the environment from the condensers. The box (base, walls and gutters) is made of fiberglass due to its low thermal conductivity of 0.04 W/m-K and manufactured in one piece to minimizes liquid losses due to leaks. The absorber was made with a mixture of silicone and iron-manganese oxides at 2.3% wt due to its mechanical stability and easy production, having a solar absorptance of 91.82% and an average emittance of 57.22% The inclination of the roofs is 16° and the height of the water mirror is between 1 cm and 4 cm thick to ensure the fast evaporation desired in the technique. Fig.6 shows a scheme of the solar distillation experimental prototype.

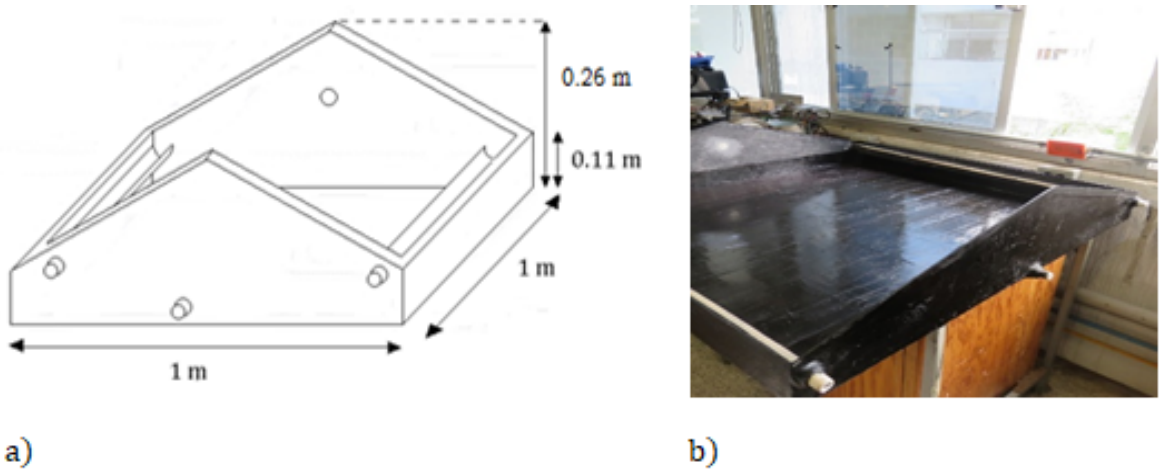

Fig. 6 a) Schematic diagram of the two-slope fiberglass still. b) Fe_2O_3:Mn/silicon hybrid solar absorber picture, applied to the bottom of the solar still.

3.5. Efficiency

The calculation of thermal efficiency is carried out by dividing the useful heat throughout the day and the total insolation H received (see equations 5 and 6) so it is necessary to quantify the water production per hour, the latent evaporative heat as a function of the temperature, as well as the radiation received from the sun at each hour of the day. Figure 7 shows the temperature of the solar absorber, the east and west condenser (Figure a) as well as the irradiance throughout the day (Figure b) for some days in March.

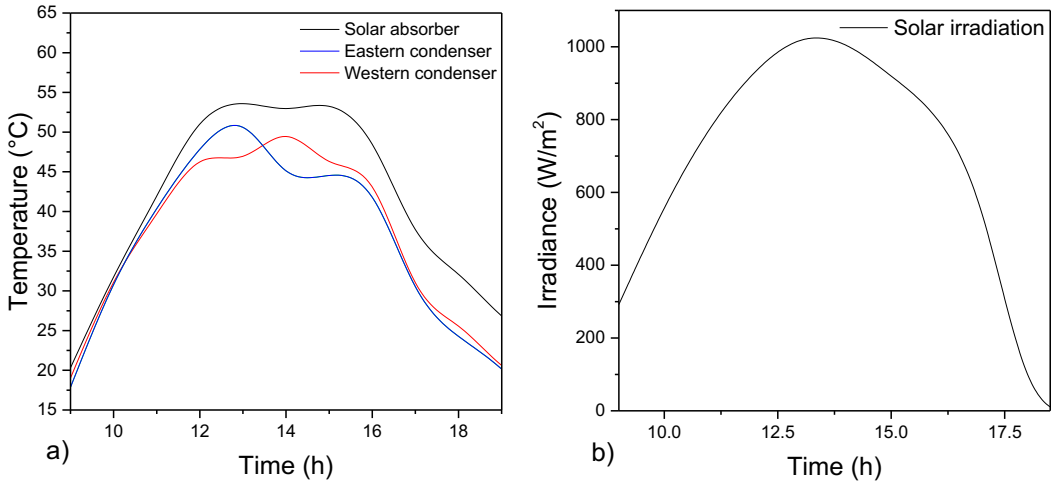

Fig. 7 a) Temperature values in the solar absorber and condensers for each hour. b) Solar irradiance for each hour.

Figure 8 shows the hourly distilled water production (Figure a) and the cumulative distilled water production (Figure b) from 9:00 to 19:00.

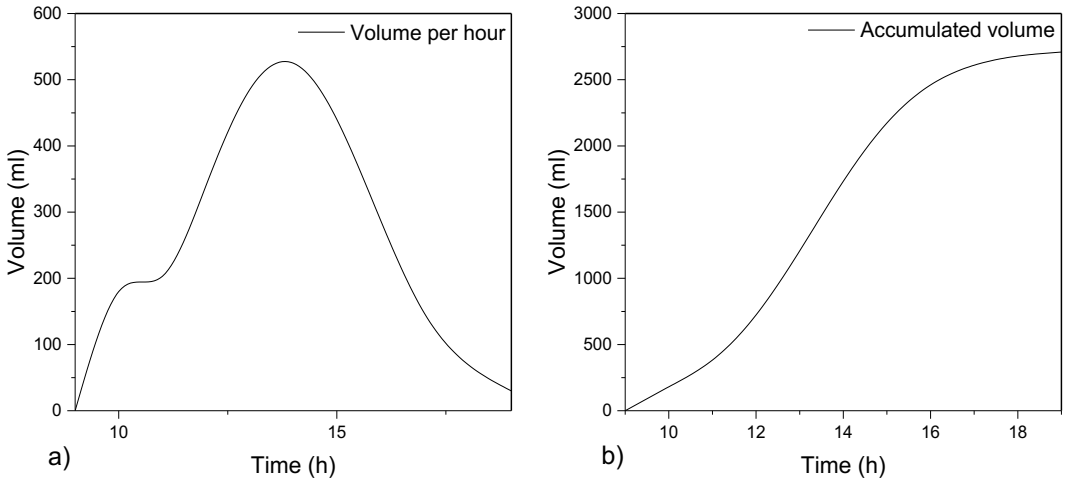

Fig. 8 a) Production of distilled water for every hour. (b) Production of accumulated distilled water for each hour.

Taking into account the above, calculations have been made for different days, the data used range from the month of October to the month of March. Table 3, by way of example, shows the values of water production, useful heat, daily insolation and efficiency of the device for some days in March, for these days, a maximum efficiency value of 27% was obtained. At this point, it is necessary to highlight the fact that the characterization of the device was carried out during the seasons of the year with less daily irradiation. Therefore, water production and efficiency will be higher during the summer.

Table 3. Useful heat, insolation and efficiency values.

Distilled water production (kg)	Useful heat per m^2(MJ/m^2)	Daily insolation H (MJ/m^2)	Thermal Efficiency η (%)
2.8	6.8	23.0	29.6

3.6. Water quality

The study consisted of comparing the inlet water to the module and the outlet water with respect to the permissible limits according to what is stipulated in the official Mexican standards [20,21]. Two types of studies were carried out: the first consisted of taking tap water and the corresponding distilled water at the exit; the second consisted of taking simulated sea water (water with 3.5% sodium chloride) and the corresponding distilled water from the prototype output.

The tests carried out for the study consisted of comparing the inlet water to the module and the outlet water with respect to the 48 parameters that NOM-127-SSA1-1994 considers to determine the quality of a water sample. Despite this, and due to the large number of studies that must be carried out to determine the quality conclusively, only the most representative parameters were selected to determine water quality through our research group, which are: smell, taste, pH, hardness, total dissolved solids, salinity, total coliforms and fecal coliforms.

For the presence of coliforms, water samples were inoculated, in different dilutions, in a series of test tubes with a Durham bell; these tubes contained lactose as a culture medium. The tubes were examined at 24 and 48 hours of incubation at 37°C. Each of those that presented turbidity with gas production were reseeded in a more selective confirmatory medium. In the case of total coliforms, the confirmatory study was made in tubes with BGBLB (Brilliant Green Bile Lactose Broth), incubated at 37°C for 48 hours. For fecal coliforms, the study was done in tubes with Escherichia coli broth (EC broth) incubated at 44.5°C for 24 hours. Using statistical tables, the most probable number (MPN) of total and fecal coliforms in 100 cm^3 of sample was calculated, from the numbers of the tubes that give positive confirmatory results [21].

Table 4 shows the results obtained in the water quality study for input samples of tap water and simulated sea water and compared with the distilled output water for each of them, as well as the maximum values accepted by NOM-127-SSA1-1994.

Table 4. Parameter data measured to determine the quality of distilled water.

Parameter	Tap water (entry)	Tap water distilled (exit)	Salt water (entry)	Water distilled (exit)	Permissible limit by NOM 127 SSA
Taste	———	Pleasurable	———	Pleasurable	Pleasant (not objectionable from a biological or chemical point of view).
Salinity (g/L)	3	3	35	3	———
Smell	———	Pleasurable	———	Pleasurable	Pleasant (not objectionable from a biological or chemical point of view).

Total Coliforms (MPN / 100ml)	23	Not detectable	180	Not detectable	Absence or undetectable
Fecal Coliforms (MPN / 100ml)	Not detectable	Not detectable	27	Not detectable	Absence or undetectable
pH	8.6	7.8	7.9	7.3	6.5-8.5
TDS (mg/L)	861	13	9370	11	1000
Water Hardness (mg/L)	450	20	550	20	500

As presented in Table 4, each of the parameters is within the norm. Preliminarily and with regard to these studies, the water is appropriate for human consumption, since not only are the imposed limits not exceeded, but also each parameter is well below what is permissible; however, it must be emphasized that in order to have a convincing characterization it is necessary to evaluate each parameter of the update of NOM-127-SSA1-1994.

4. Conclusions

This research has made it possible to obtain a sustainable, low-cost, easy-to-maintain prototype with a thermal efficiency of 29.6%. This efficiency was achieved with the solar absorber of 2.3% Mn-Fe oxides, with an absorptance of 91.82% and an emittance of 57.22% and with an average condenser transmittance of 82.59%. In terms of daily water production, the device produces an average of 2.8 L of water. Regarding the quality of distilled water, for the two water samples studied corresponding to tap water and simulated sea water, the measured parameters are below the values required by the Mexican standard NOM-127-SSA1-1994. In the bacteriological studies, neither total coliforms nor fecal coliforms were detected for both distilled water from tap water and for distilled water from simulated sea water. The high quality of water distilled by means of solar stills suggests that it should be considered a priority due to its great energy and environmental relevance. It is of great importance to continue the study of passive solar distillation from the perspective of improving thermal efficiency, sizing and exergetic studies that allow increasing daily water production.

Acknowledgments

The support provided by the National Council of Science and Technology (CONACYT, Mexico) through project No. 60781 and the PEMA, belonging to the national register of postgraduate courses CONACYT (agreement 003893) is appreciated. Víctor Rentería is grateful to the CONACYT.

Credit author statement

Barrera C, E: Conceptualization, Methodology, Software, Supervision and Project administration. **Renteria T. V**: Experimental Methodology. **Juarez S, C**: Investigation, Formal analysis, Visualization and Writing. **Fernández R, C**: Resources and Investigation. **Ventura R, R**: Writing and Revision.

References.

[1] Y. Zhang, M. Sivakumar, S. Yang, K. Enever, M. Ramezanianpour, Application of solar energy in water treatment processes: A review. *Desalination*, 428(2018), 116-145, https://doi.org/10.1016/j.desal.2017.11.020

[2] M. N. I. Sarkar, A. I. Sifat, S. S. Reza, M. S. Sadique, A review of optimum parameter values of a passive solar still and a design for southern Bangladesh, *Renewables: Wind, Water, and Solar*, *4*,1(2017) 1-13, https://doi.org/10.1186/s40807-017-0038-8

[3] K. H. Nayi, K. V. Modi, Pyramid solar still: A comprehensive review, *Renewable and Sustainable Energy Reviews*, 81(2018), 136-148, https://doi.org/10.1016/j.rser.2017.07.004

[4] I. Altarawneh, M. Batiha, S. Rawadieh, M. Alnaief, M. Tarawneh, Solar desalination under concentrated solar flux and reduced pressure conditions, *Solar Energy*, 206(2020) 983-996, https://doi.org/10.1016/j.solener.2020.06.058

[5] K. K. Murugavel, P. Anburaj, R. S. Hanson, T. Elango, Progresses in inclined type solar stills, *Renewable and sustainable energy reviews*, 20(2013) 364-377, https://doi.org/10.1016/j.rser.2012.10.047

[6] M. M. Thalib, A. M. Manokar, F. A. Essa, N. Vasimalai, R. Sathyamurthy, F. P. Garcia-Marquez, Comparative study of tubular solar stills with phase change material and nano-enhanced phase change material, *Energies*, 13, 15 (2020) 3989, https://doi.org/10.3390/en13153989

[7] K. V. Modi, K. H. Nayi, S. S. Sharma, Influence of water mass on the performance of spherical basin solar still integrated with parabolic reflector, *Groundwater for Sustainable Development*, 10(2020) 100299, https://doi.org/10.1016/j.gsd.2019.100299

[8] A. E. Kabeel, S. A. El-Agouz, Review of researches and developments on solar stills, *Desalination*, 276, 1-3, (2011) 1-12, https://doi.org/10.1016/j.desal.2011.03.042

[9] F. Muñoz, E. Barrera, A. Ruiz, E. M. Martínez, N. Chargoy, Long-term experimental theoretical study on several single-basin solar stills, *Desalination*, *476*(2020), 114241, https://doi.org/10.1016/j.desal.2019.114241

[10] T. Arunkumar, J. Wang, D. D. W. Rufuss, D. Denkenberger, A. E. Kabeel, Sensible desalting: Investigation of sensible thermal storage materials in solar stills, *Journal of Energy Storage*, 32(2020), 101824, https://doi.org/10.1016/j.est.2020.101824

[11] K. Selvaraj, A. Natarajan, Factors influencing the performance and productivity of solar stills-A review, *Desalination*, 435(2018), 181-187, https://doi.org/10.1016/j.desal.2017.09.031

[12] S. Wijewardane, D. Y. Goswami, A review on surface control of thermal radiation by paints and coatings for new energy applications, *Renew. Sustain. Energy Rev. 16*(2012), 1863-1873. https://doi.org/10.1016/j.rser.2012.01.046

[13] C.D. Hernández-Pérez, E. Barrera-Calva, F. González, V. Rentería Tapia, Ultrasonic spray pyrolysis technique to generate a solar absorber coating of Mn-doped α-Fe2O3, Renew. Energy Environ. Sustain. 6 (2021). https://doi.org/10.1051/rees/2021003

[14] M. K. Estahbanati, A. Ahsan, M. Feilizadeh, K. Jafarpur, S. S. Ashrafmansouri, M. Feilizadeh, Theoretical and experimental investigation on internal reflectors in a single-slope solar still, *Appl. energy*, 165(2016), 537-547, https://doi.org/10.1016/j.apenergy.2015.12.047

[15] T. Rajaseenivasan, R. Prakash, K. Vijayakumar, K. Srithar, Mathematical and experimental investigation on the influence of basin height variation and stirring of water by solar PV panels in solar still, *Desalination*, 415(2017), 67-75, https://doi.org/10.1016/j.desal.2017.04.010

[16] Conagua Programa Nacional Hídrico 2014-2018, México, DF: Comisión Nacional del Agua, (2014), Retrieved from http://www.conagua.gob.mx/conagua07/contenido/documentos/PNH2014-2018.pdf.

[17] Duffie, J. A., Beckman, W. A., & Blair, N. (2020). Solar engineering of thermal processes, photovoltaics and wind. John Wiley & Sons.

[18] De Maio, D., D'Alessandro, C., Caldarelli, A., De Luca, D., Di Gennaro, E., Russo, R., & Musto, M. (2021). A selective solar absorber for unconcentrated solar thermal panels. Energies, 14(4), 900. https://doi.org/10.3390/en14040900

[19] M.A.S. Malik, G.N. Tiwari, A. Kumar, M.S. Sodha, Solar distillation: a practical study of a wide range of stills and their optimum design, construction, and performance, New York, EUA: Pergamon Press, (1982).

[20] NORMA Oficial Mexicana NOM-127-SSA1-1994, Salud ambiental, Agua para uso y consumo humano, Límites permisibles de calidad y tratamientos a que debe someterse el agua para su potabilización, (1994).

[21] NORMA Oficial Mexicana NOM-210-SSA1-2014 Productos y servicios. Métodos de prueba microbiológicos, Determinación de microorganismos indicadores. Determinación de microorganismos patógenos, (2014).